Eur. Phys. J. B **16**, 157–168 (2000)

THE EUROPEAN PHYSICAL JOURNAL B

EDP Sciences

Thermal convection in a rotating layer of a magnetic fluid

G.K. Auernhammer[a] and H.R. Brand

Theoretische Physik III, Universität Bayreuth, 95540 Bayreuth, Germany

Received 10 November 1999

Abstract. Thermal convection in magnetic fluids can be driven by buoyancy or by magnetic forces (due to the thermomagnetic effect). Depending on the direction of the applied temperature gradient, buoyancy effects can be stabilizing (heating from above) or destabilizing (heating from below), whereas the magnetic forces always play a destabilizing role for magnetic fields perpendicular to the interface. We investigate the influence of rotations using both linear and weakly non-linear analyses of the governing hydrodynamic equations in the Boussinesq approximation. With a linear stability analysis we determine the values of the wavelength and the temperature gradient at the onset of convection (critical values). These are calculated analytically in the case of stress free boundaries and numerically for rigid boundaries. We discuss the validity of the assumptions entering the calculations for stress free boundaries. In the case of free boundary conditions, asymptotic expressions of the critical values for high rotation rates are derived. When the system is heated from above and the magnetic forces only slightly exceed the buoyancy forces, linear results show that both the critical wavelength and the critical temperature gradient diverge. Again, this behavior is described by asymptotic expressions. We derive envelope equations for convection patterns characterized by both: one wave vector and two competing wave vectors of equal length but different directions. These equations show that the system always exhibits a forward bifurcation. The well-known Küppers-Lortz instability is also present in magnetic fluids. This instability sets in at critical values for a sufficiently high rotation rate. In simple fluids the angle α depends only on the Prandtl number of the fluid. We show that for magnetic fluids this angle can be changed by changing the ratio of the buoyancy forces to the magnetic forces (*i.e.* by changing the magnetic field). There is also a weak dependence on the other magnetic parameters of the system. For a commercially available magnetic fluid this angle can be increased by approximately $10^\circ - 15^\circ$ compared to the simple fluid case.

PACS. 75.50.Mm Magnetic liquids – 47.54.+r Pattern selection; pattern formation – 05.70.Ln Nonequilibrium and irreversible thermodynamics

1 Introduction

Convection in a rotating layer of a fluid is an intensely studied field, however there remain many open questions. To start with the simplest case, consider a layer of a simple fluid heated from below. Everyday experience shows that the thermally conductive ground state of this system becomes unstable to a convective state as the temperature difference between the top and the bottom of the fluid layer rises above a certain critical value. A broad overview of the state of knowledge on convection phenomena in a layer of simple fluid was given by Chandrasekhar [1]. Beyond the linear analysis summarized by Chandrasekhar Schlüter, Lortz and Busse [2] performed pioneering work using a weakly nonlinear analysis of the equations governing a non-rotating fluid layer heated from below. They showed that, within a certain area in parameter space, convection rolls are stable just above the onset of convection. For convection in a rotating layer of a simple fluid, Küppers and Lortz [3] predicted an instability of the convection pattern at onset to a similar pattern which is rotated by a certain angle with respect to the initial pattern, if the rotation rate exceeds a certain critical value. Thus the Küppers-Lortz (KL) instability gives the opportunity to study complex pattern dynamics in a parameter range in which a weakly nonlinear analysis should be valid. Busse and Heikes [4] observed the KL instability experimentally and found an angle close to 60°, which is in good agreement with theoretical predictions. Over the last decade renewed interest in the KL instability grew [5–11]. The experimental work shows several features which are not covered by the weakly nonlinear theory. Among these are: KL instability may set in for values less than the critical rotation rate if the applied temperature gradient is sufficiently larger than the critical temperature gradient. The switching angle found experimentally at rotation rates above critical is usually close to 60° [4,10]. The theoretical predictions range from 10° to 60° depending on the Prandtl number of the fluid [7,10] and differ from those experimentally found [9,10].

[a] e-mail: btpb03@theo.phy.uni-bayreuth.de

Magnetic fluids (often called ferrofluids) are colloidal suspensions of small magnetic monodomain particles (their diameter is typically 10 nm) in a carrier fluid. In an applied field these fluids react like super-paramagnets with a susceptibility at low fields of up to 10. Since the magnetic potential energy of the magnetic particles in typical fields (up to a few 10^{-2} T) is comparable to the thermal energy kT, the magnetization of these fluids depends strongly on temperature. For a detailed introduction to magnetic fluids see [12–15]. Placed in a magnetic field, a magnetic fluid experiences a body force, usually written as the Kelvin force $\mu_0 \mathbf{M} \cdot \nabla \mathbf{H}$. We note that there is still a controversy on the correct formulation of this body force (see *e.g.* [16]); however, the discussed formulations are equivalent in the approximations we make in this paper (see below). The dependence of the magnetization on temperature leads to a second driving mechanism for convection [17]. As we explain below, magnetically driven convection occurs when the system is heated from below *or* above. Finlayson [17] and later Gotoh and Yamada [18] analyzed linear convection in a non-rotating layer (horizontally unbounded) of a magnetic fluid. Schwab and coworkers verified their results experimentally and visualized the flow pattern [19–21]. However, they had to apply an additional magnetic field in the plane of the layer to align the convection rolls. In the absence of this longitudinal field they found an irregular convection pattern. Further theoretical investigations on the problem were done by Stiles, Blennerhassett and co-workers [22–25]. They showed that the critical temperature difference and the critical wave number of the convection pattern at the onset of convection may increase drastically if the system is heated from above [23,25]. In their nonlinear analysis of the system they concentrated mainly on the heat transfer through the layer [23–25]. Using weakly nonlinear analysis Bajaj and Malik [26] concluded that straight convection rolls are stable just above the onset of convection in the case of stress free boundaries. All this theoretical work was done assuming non-deformable boundaries of the fluid layer. Quite recently Weilepp and Brand [27] showed that the convection rolls interact with the normal field surface instability (Rosensweig instability [28]) of magnetic fluids if the upper boundary is assumed to be deformable.

We note that there are some other systems to which the analysis presented in the following applies. Convection in paramagnetic liquids under strong magnetic fields [29,30] as well as in dielectric liquids under electric fields [31] is governed by an isomorphic set of equations if the same geometry is considered. In the latter case, however, the convection mechanism due to the Kelvin force is frequently altered substantially by various other mechanisms if free charge carriers (electrons and ions) are present, due to impurities.

Here we study for the first time, linearly and weakly nonlinearly, the influence of rotation on the onset of thermal convection in a magnetic fluid. In particular we investigate how the KL instability is altered on going from the simple fluid limit to the magnetic dominated convection. We demonstrate that the KL angle can be tuned in this system continuously by changing the magnetic field and varied in total over more than 10 degrees.

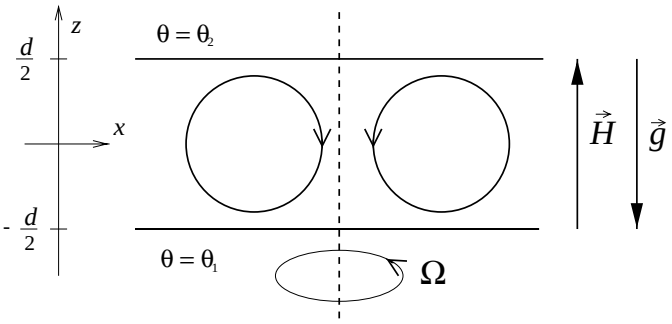

Fig. 1. A vertical cut through the fluid layer. Note the y-axis points into the xz-plane.

The paper is organized as follows. After a brief outline of the system under investigation and its convection mechanisms we present the mathematical description (Sect. 2). In Section 3 we perform a linear stability analysis which will be the basis of the investigation of the Küppers-Lortz instability in Section 4.

2 Convection mechanisms and their mathematical formulation

Figure 1 gives a schematic overview of the geometry investigated. We consider a layer of a magnetic fluid of constant thickness d parallel to the xy-plane with no lateral boundaries. The upper and lower boundaries are situated at $z = \pm\frac{d}{2}$. The temperatures θ_1 and θ_2 are applied to the lower and upper boundaries, respectively. The whole layer can rotate about the z-axis with an angular velocity Ω. Gravity acts in negative z-direction: $\mathbf{g} = -g\hat{\mathbf{e}}_z$. The setup is assumed to be placed in a magnetic field $\mathbf{H}$ parallel to $\hat{\mathbf{e}}_z$, which would be homogeneous if the magnetic fluid were absent.

Magnetic fluids can be modeled as liquid non-conducting super-paramagnets [14,17,18,23]. In such a model we have to solve the Maxwell equations simultaneously with the balance equations of entropy (heat equation), linear momentum (Navier-Stokes equation) and mass (continuity equation). Since the fluid is assumed to be insulating, the Maxwell equations reduce to

$$\nabla \cdot \mathbf{B} = 0 \tag{1}$$

$$\nabla \times \mathbf{H} = 0. \tag{2}$$

Because of equation (2) we can express the magnetic field by a scalar potential

$$\mathbf{H} = -\nabla\phi. \tag{3}$$

The viscous stress tensor entering the Navier-Stokes equation has to be extended by a suitable magnetic part.

Table 1. Physical parameters of the magnetic fluid EMG 905 produced by Ferrofluidics.

density ρ $\left[\frac{\mathrm{kg}}{\mathrm{m}^3}\right]$	1.24×10^3
kinematic viscosity (27°C) ν $\left[\frac{\mathrm{m}^2}{\mathrm{s}}\right]$	12×10^{-6}
thermal diffusivity κ $\left[\frac{\mathrm{m}^2}{\mathrm{s}}\right]$	8×10^{-8}
heat capacity c_p $\left[\frac{\mathrm{J}}{\mathrm{kg\,K}}\right]$	1.47×10^3
coefficient of volume expansion α $\left[\frac{1}{\mathrm{K}}\right]$	8.6×10^{-4}
susceptibility at low field χ	1.9
pyromagnetic coefficient at $H = 50\frac{\mathrm{kA}}{\mathrm{m}}$ $\left[\frac{\mathrm{A}}{\mathrm{Km}}\right]$	110
mean particle diameter [nm]	10.2

For this contribution we will use the formulation of the magnetic stress tensor proposed by Rosensweig [14]:

$$\mathsf{T}_\mathrm{m} = \left[\mu_0 \int_0^H \left(\frac{\partial(M\mathrm{v})}{\partial \mathrm{v}}\right)_{\theta,H} \mathrm{d}H + \frac{\mu_0}{2} H^2\right] \mathsf{I} + \mathbf{BH}, \quad (4)$$

where μ_0 is the magnetic permeability of vacuum, M the magnetization of the fluid, v the specific volume, I the unity tensor and $\mathbf{B}$ the magnetic induction. This stress tensor significantly simplifies by assuming that the magnetization of the fluid can be written in the form

$$\mathbf{M} = [M_0 + \chi(H - H_0) - K(\theta - \theta_0)]\hat{\mathbf{e}}_z, \quad (5)$$

where $M_0 = M(H_0, \theta_0)$ (H_0 and θ_0 are the values in the middle of the layer), χ is the magnetic susceptibility and K is the pyromagnetic coefficient (see Tab. 1 for a set of data of a commercially available magnetic fluid [27,32]). Using this approximation, the gradient of T_m reduces to the magnetic Kelvin force $\mu_0 M \nabla H$ plus a pressure like term [14] so the Navier-Stokes equation in a corotating frame reads:

$$\rho\frac{\partial \mathbf{v}}{\partial t} + \rho\mathbf{v}\cdot\nabla\mathbf{v} = -\nabla\tau + \rho\mathbf{g} + \mu_0 M \nabla H + \eta\nabla^2\mathbf{v} + 2\rho\mathbf{v}\times\boldsymbol{\Omega}, \quad (6)$$

with the velocity field $\mathbf{v} = (v_x, v_y, v_z)$, the viscosity η, the mass density ρ and a modified pressure τ, which includes all terms that can be written as gradients. Throughout our analysis we will assume that the rotation rate is small and the effective $\mathbf{g}$ stays parallel to the z-axis. Neglecting viscous dissipation, the heat equation in magnetic fluids reads (see *e.g.* Refs. [17,33]):

$$\left[\frac{\partial}{\partial t} + \mathbf{v}\cdot\nabla\right]\theta + \frac{\mu_0\theta K}{\rho C}\left[\frac{\partial}{\partial t} + \mathbf{v}\cdot\nabla\right]\partial_z\phi = \kappa\nabla^2\theta, \quad (7)$$

where C is a modified heat capacity and κ the thermal diffusivity. Inserting typical values shows that the ϕ-term on the left hand side is small compared to the other terms. For this reason we will neglect it in our further calculations.

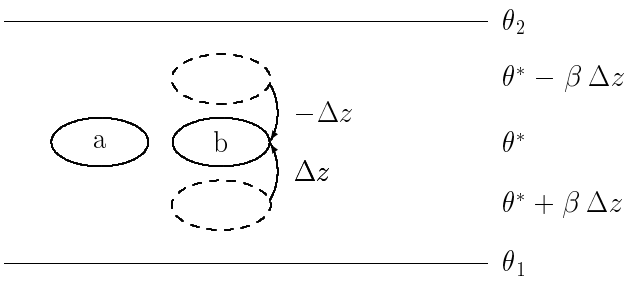

Fig. 2. A displaced fluid particle experiences a force. If the force points in the direction of the displacement the layering might be unstable.

The boundaries are assumed to be ideal thermal conductors, thus the temperature of the fluid at the boundaries is identical to the applied temperature. For the velocity field we deal with both (stress-) free boundaries (to obtain closed analytical expressions as results)

$$0 = \hat{\mathbf{e}}_x \cdot (\hat{\mathbf{n}} \cdot \mathsf{T}) = \hat{\mathbf{e}}_y \cdot (\hat{\mathbf{n}} \cdot \mathsf{T}) \quad (8)$$

$$0 = v_z \quad (9)$$

where T is the stress tensor and rigid (experimental) boundaries (to give concrete predictions for experiments)

$$0 = \mathbf{v}. \quad (10)$$

Last but not least, the magnetic field and the magnetic induction have to fulfill the usual continuity conditions.

$$0 = \hat{\mathbf{e}}_z \cdot (\mathbf{B}_\mathrm{int.} - \mathbf{B}_\mathrm{ext.}) \quad (11)$$

$$0 = \hat{\mathbf{e}}_z \times (\mathbf{H}_\mathrm{int.} - \mathbf{H}_\mathrm{ext.}). \quad (12)$$

One easily sees that a pure conductive state fulfills the governing equations. Using the averaged temperature gradient $\beta = \frac{\theta_1 - \theta_2}{d}$ (β is positive if the lower plate is warmer than the upper one), this conductive state is given by:

$$\mathbf{v} = 0 \quad (13)$$

$$\theta = \theta_0 - \beta z \quad (14)$$

$$M = M_0 + \frac{K\beta z}{1+\chi} \quad (15)$$

$$H = H_0 - \frac{K\beta z}{1+\chi}, \quad (16)$$

with an unperturbed magnetic field outside the layer.

Before presenting our results we will highlight an important difference between the driving forces involved in convection in a magnetic fluid (see Fig. 2). Consider two fluid particles, one (b) displaced by a distance Δz in the layer (but leaving its internal properties — such as temperature and density — unchanged), and the other (a) kept at its initial position (thus having the equilibrium

properties given by Eqs. (13) through (16)). The resulting force density $\mathbf{f}$ on the displaced particle is given by the difference between the force densities on particles (b) and (a) $\mathbf{f} = \mathbf{f}_\mathrm{b} - \mathbf{f}_\mathrm{a}$. If this force density points in the direction of the displacement, the layering might be unstable, otherwise it is stable. Evaluating this expression for buoyancy ($\mathbf{f} \sim \beta\, \Delta z\, \hat{\mathbf{e}}_z$) and the magnetic Kelvin force ($\mathbf{f} \sim \beta^2\ \Delta z\ \hat{\mathbf{e}}_z$) shows a significant difference: whereas buoyancy is only destabilizing when the layer is heated from below ($\beta > 0$), the Kelvin body force is always destabilizing independent of the sign of the applied temperature gradient β.

Heat conduction and viscous dissipation always stabilize the layering and counteract these driving forces. For small applied temperature gradients, the dissipative, stabilizing, mechanisms will dominate the behavior of the system and equations (13) through (16) hold. Above a certain temperature gradient (called the critical temperature gradient) the layering in the sample is unstable and increasing thermal fluctuations can lead to convection. In the following section we will determine the threshold values at which convection sets in.

3 Linear stability analysis

3.1 Dimensionless equations

To write the governing equations in dimensionless form we introduce characteristic scales: d for length, $\frac{d^2}{\kappa}$ for time, βd for temperature, $\frac{K\beta d^2}{1+\chi}$ for magnetic potential and $\frac{\kappa}{d}$ for velocity. Since the magnetic fluid will, in general, alter the magnetic field outside the fluid layer, we have to solve the Maxwell equations in the whole space. For this reason we use Φ_e, the magnetic potential outside the fluid layer, as an additional variable. Furthermore we add to the conductive solutions small perturbations (*e.g.* $\theta \rightarrow \theta + \theta'$). In these dimensionless units the governing equations for the perturbations take in the Boussinesq approximation, the form (in a corotating frame and after dropping the primes):

$$\frac{1}{P}\left[\frac{\partial}{\partial t} + \mathbf{v}\cdot\nabla\right]\mathbf{v} = -\nabla\tau + R(1+M_1)\theta\hat{\mathbf{e}}_z + \nabla^2\mathbf{v} + \sqrt{T}\mathbf{v}\times\hat{\mathbf{e}}_z + RM_1\partial_z\phi\hat{\mathbf{e}}_z + RM_1\theta\nabla\partial_z\phi \quad (17)$$

$$\left[\frac{\partial}{\partial t} + \mathbf{v}\cdot\nabla\right]\theta = \nabla^2\theta \quad (18)$$

$$0 = \nabla\cdot\mathbf{v} \quad (19)$$

$$0 = [\partial_{zz} + M_3(\partial_{xx}+\partial_{yy})]\phi + \partial_z\theta \quad (20)$$

$$0 = \nabla^2\phi_\mathrm{e}. \quad (21)$$

In equations (17–21) the external parameters are measured by the following dimensionless quantities (see Tab. 2 for the explicit definitions): the Rayleigh number R represents the dimensionless temperature gradient, the dimensionless rotation rate is incorporated in the Taylor number T (which is proportional to the square of the angular velocity), the ratio between the magnetic force and the buoyancy is measured by the constant M_1, M_3 is a measure of the deviation of the magnetization curve from the linear behavior $M_0 = \chi H_0$, and the Prandtl number P is the ratio between the kinetic viscosity and the thermal diffusivity.

We note that some authors use instead of T, the dimensionless rotation rate $\Omega_0 = \frac{d^2}{\nu}\Omega$, which is connected to T *via* $T = 4\ {\Omega_0}^2$. Using the equations in this form includes two dependent variables: the pressure τ and one component of the velocity field could easily be eliminated by applying $\nabla\times$ and $\nabla\times\nabla\times$ to the Navier-Stokes equation and then considering only the z component of the resulting equations. We will keep all variables for completeness. The equation governing rotating convection in simple fluids are obtained in the limit $M_1 \rightarrow 0$ and $M_3 = 1$. Later on we will refer to the governing equations in the form

$$\mathcal{L}u + \mathcal{N}(u|u) = 0, \quad (22)$$

where $u = (v_x, v_y, v_z, \theta, \phi, \tau)$ and $\mathcal{L}$ and $\mathcal{N}$ represent, respectively, the linear and nonlinear parts of equations (17) through (20). Using $\tilde{\nabla}^2 = \partial_{zz} + M_3(\partial_{xx}+\partial_{yy})$, they can be expressed as

$$\mathcal{L} = \begin{pmatrix} \nabla^2 - \frac{1}{P}\partial_t & \sqrt{T} & 0 & 0 & 0 & -\partial_x \\ -\sqrt{T} & \nabla^2 - \frac{1}{P}\partial_t & 0 & 0 & 0 & -\partial_y \\ 0 & 0 & \nabla^2 - \frac{1}{P}\partial_t & R(1+M_1) & RM_1\partial_z & -\partial_z \\ 0 & 0 & 1 & \nabla^2 - \partial_t & 0 & 0 \\ 0 & 0 & 0 & \partial_z & \tilde{\nabla}^2 & 0 \\ \partial_x & \partial_y & \partial_z & 0 & 0 & 0 \end{pmatrix} \quad (23)$$

and

$$\mathcal{N}(u^{(p)}|u^{(q)}) = \begin{pmatrix} -\frac{1}{P}(\mathbf{v}^{(p)}\cdot\nabla)\mathbf{v}^{(q)} + RM_1\theta^{(p)}\nabla\partial_z\phi^{(q)} \\ -(\mathbf{v}^{(p)}\cdot\nabla)\theta^{(q)} \\ 0 \\ 0 \end{pmatrix}. \quad (24)$$

The boundary conditions for the perturbations now read (for a detailed derivation see *i.e.* Refs. [17,18,23]): for rigid boundaries

$$\mathbf{v}\left(z = \pm\frac{1}{2}\right) = 0, \quad (25)$$

for free boundaries

$$v_z\left(z = \pm\frac{1}{2}\right) = \partial_z v_x\left(z = \pm\frac{1}{2}\right) = \partial_z v_y\left(z = \pm\frac{1}{2}\right) = 0, \quad (26)$$

Table 2. The dimensionless parameters introduced in equations (17–21). In these definitions α denotes the coefficient of volume expansion and ν the kinematic viscosity.

parameter	notation	definition
Rayleigh number (temperature gradient)	R	$\frac{\alpha\beta g d^4}{\nu\kappa}$
Prandtl number	P	$\frac{\nu}{\kappa}$
Taylor number (rotation parameter)	T	$4\frac{d^4}{\nu^2}\Omega^2$
strength of magnetic force relative to buoyancy	M_1	$\frac{\mu_0 K^2 \beta}{(1+\chi)\alpha\rho g}$
nonlinearity of magnetization	M_3	$\frac{1+\frac{M_0}{H_0}}{1+\chi}$

and, independent of the velocity boundary conditions,

$$\theta\left(z=\pm\frac{1}{2}\right)=0 \tag{27}$$

$$\phi\left(z=\pm\frac{1}{2}\right)=\phi_{\mathrm{e}}\left(z=\pm\frac{1}{2}\right) \tag{28}$$

$$(1+\chi)\partial_z\phi\left(z=\pm\frac{1}{2}\right)=\partial_z\phi_{\mathrm{e}}\left(z=\pm\frac{1}{2}\right). \tag{29}$$

As already mentioned above, the fact that closed analytical results allow a more direct insight to the physical mechanisms to be gained, motivated our use of free boundary conditions. From the experimental point of view free boundary conditions usually coincide with deformable boundaries and this gives rise to surface instabilities [28] which can interact with the convection patterns [27]. A full analysis of the problem with free and deformable boundaries is beyond the scope of this article and we will restrict ourselves to the case of free but fixed boundaries.

3.2 Solutions to the linearized equations

When convection sets in, thermal noise with a certain wave number is no longer overdamped and can grow. With linear considerations it is sufficient to deal with each wave number separately. For example our ansatz for the vertical component of the velocity field reads:

$$v_z = W(z)\exp(\lambda t + \mathrm{i}ax) + \mathrm{c.c.}, \tag{30}$$

where we set the wave vector **a** of the convection rolls to be parallel to the x-axis. The time dependence $\exp(\lambda t) = \exp[(\sigma+\mathrm{i}\omega)t]$ includes both the growth rate σ and a possible oscillation with a frequency $\frac{\omega}{2\pi}$. If the layering is stable, the growth rate σ is negative for all wave vectors. Just above convective onset, σ becomes positive for a small band of wave numbers. Looking for the onset of stationary convection we set $\sigma = 0$. First we deal with stationary convection setting $\omega = 0$; later in this section we will also investigate the case $\omega \neq 0$. For all unknown functions (v_x, v_y, θ, ϕ, ϕ_{e} and τ) ansätze similar to equation (30) are made. Since convection rolls are expected as a first instability, the functions should have the symmetries, with respect to inversion of the z-axis, shown in Table 3.

Table 3. The symmetry of all relevant functions under inversion of the z-axis.

function	notation for z dependence	z-symmetry
v_z	$W(z)$	even
v_x	$U(z)$	odd
v_y	$V(z)$	odd
θ	$\Theta(z)$	even
ϕ	$\Phi(z)$	odd
τ	$P(z)$	odd

3.2.1 Free boundaries

In the case of free boundaries, it can easily be shown [1] that all even derivatives of $W(z)$ must vanish. Thus we let

$$W(z) = \cos(\pi z). \tag{31}$$

Although equations (28, 29) hold for both rigid and free boundaries, we have to restrict ourselves to the limiting case $\chi \to \infty$, because this is the only possibility to continue with this simple analytical ansatz. Later on we will show the cases for which these results differ from results for experimentally accessible values of χ. Inserting equation (31) in the linearized governing equations (22)

$\mathcal{L}u = 0$ leads to

$$U(z) = -\mathrm{i}\frac{\pi}{a}\sin(\pi z) \tag{32}$$

$$V(z) = -\mathrm{i}\frac{\sqrt{T}\pi}{a(\pi^2+a^2)}\sin(\pi z) \tag{33}$$

$$W(z) = \cos(\pi z) \tag{34}$$

$$\Theta(z) = \frac{1}{\pi^2+a^2}\cos(\pi z) \tag{35}$$

$$\Phi(z) = -\frac{\pi}{(\pi^2+a^2)(\pi^2+a^2M_3)}\sin(\pi z). \tag{36}$$

The dependence on the horizontal coordinates is given in equation (30). Since $P(z)$ and $\Phi_\mathrm{e}(z)$ do not enter into further calculations we do not give them explicitly. If rotation was absent, one would expect a two-dimensional flow field with vanishing $V(z)$. In rotating convection however, such a flow field is impossible due to the Taylor-Proudman theorem [1]. For a non-viscous fluid this theorem predicts (for the geometry investigated here) a two-dimensional flow field which lies in the plane perpendicular to the axis of rotation. Since we deal with viscous fluids the Taylor-Proudman theorem holds only in the limit of large rotation rates. For small rotation rates (small T), $V(z)$ is negligible and the flow field lies in the xz-plane, but for large T v_y is the dominant component of the velocity. As solvability condition to the linear part of equation (22) we find

$$R = \frac{(\pi^2+a^2M_3)}{(1+M_1)(\pi^2+a^2M_3)-M_1\pi^2}\ \frac{T\pi^2+(\pi^2+a^2)^3}{a^2}, \tag{37}$$

which is the analytical form of the curve of marginal stability (the region below the curve corresponds to the conductive state and the region above to the convective state of the system). Note the similarity to the corresponding formula in the simple fluid case: the critical Rayleigh number can be factorized in a non-magnetic part (the second fraction is the well known result for simple fluids [1]) and a magnetic part. The values of the Rayleigh number and the wave number at the onset of convection (R_c and a_c) result from a minimization of R (Eq. (37)) with respect to a. These critical values depend on the system parameter M_1, M_3 and T. Figure 3 gives an overview of the critical values as a function of the rotation rate (T) and the relative strength of the magnetic forces (M_1). These plots show two distinct regimes. At low rotation rates both the critical wave number a_c and the critical Rayleigh number R_c depend only the magnetic parameters and are almost independent of T. At high T all critical values follow universal power laws. We will derive and discuss these power laws in Section 3.3.

Let us remark that making the same calculation for a possible oscillatory instability ($\omega \neq 0$) leads to, besides a somewhat modified version of equation (37), a second condition of solvability:

$$\frac{\omega^2}{P^2} = \frac{1-P}{1+P}\ \frac{T\pi^2}{\pi^2+a^2} - (\pi^2+a^2)^2. \tag{38}$$

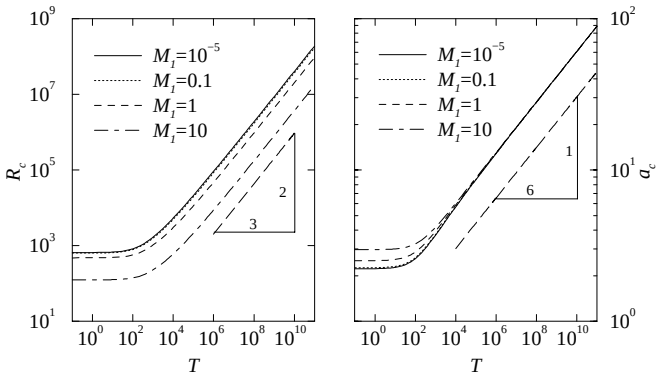

Fig. 3. Overview of the critical Rayleigh numbers (left) and wave numbers (right) for free boundaries and various magnetic parameters as a function of T. The parameter $M_3 = 1$ was chosen for the smallest M_1 and $M_3 = 1.1$ in all other cases. For a detailed discussion of the fit see Section 3.3.

One easily sees that this condition can only be fulfilled for Prandtl numbers smaller than unity. Thus, for free boundaries, oscillatory convection can be ruled out for all commercially available magnetic fluids.

3.2.2 Rigid boundaries

The boundary conditions for rigid boundaries do not allow simple solutions as in the case of free boundaries. In this work we solve the linearized equations $\mathcal{L}u = 0$ by linear combination of exponential functions (see Refs. [1,7]). With respect to the symmetries summarized in Table 3, these functions now read

$$W(z) = \sum_{j=1}^{n} B_j w_j \frac{\cosh(q_j z)}{\cosh\left(\frac{q_j}{2}\right)} \tag{39}$$

$$\Theta(z) = \sum_{j_1}^{n} B_j t_j \frac{\cosh(q_j z)}{\cosh\left(\frac{q_j}{2}\right)} \tag{40}$$

$$\Phi(z) = \sum_{j=1}^{n} B_j f_j \frac{\sinh(q_j z)}{\sinh\left(\frac{q_j}{2}\right)} \tag{41}$$

$$\Phi_\mathrm{e}(z) = \begin{cases} B_{n+1}\dfrac{\exp(-a|z|)}{\exp\left(-\frac{a}{2}\right)} & \text{for } z > 0 \\ -B_{n+1}\dfrac{\exp(-a|z|)}{\exp\left(-\frac{a}{2}\right)} & \text{for } z < 0 \end{cases} \tag{42}$$

and analogous formulas for horizontal components of the velocity field and the pressure can be derived. In equations (39–41) we introduced the following notations: q_j are the roots of the characteristic polynomial Q associated with $\mathcal{L}$

$$Q = \Big\{ -(q^2-a^2M_3)\left[(q^2-a^2)^3 + Tq^2 + a^2R(1+M_1)\right] + a^2RM_1q^2 \Big\}(q^2-a^2). \tag{43}$$

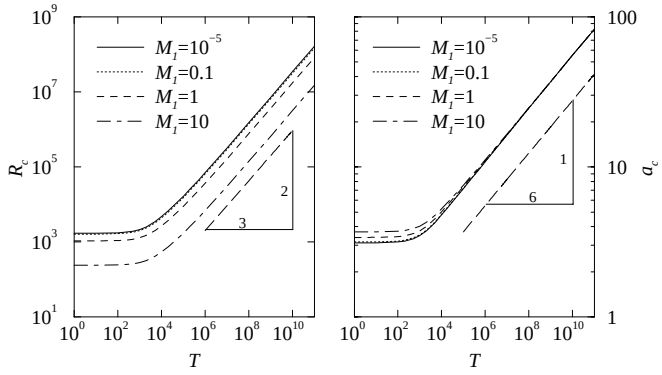

Fig. 4. Overview of the critical Rayleigh numbers (left) and wave numbers (right) for rigid boundaries and various magnetic parameters as a function of T (magnetic parameters as in Fig. 3). For a detailed discussion of the fit see Section 3.3.

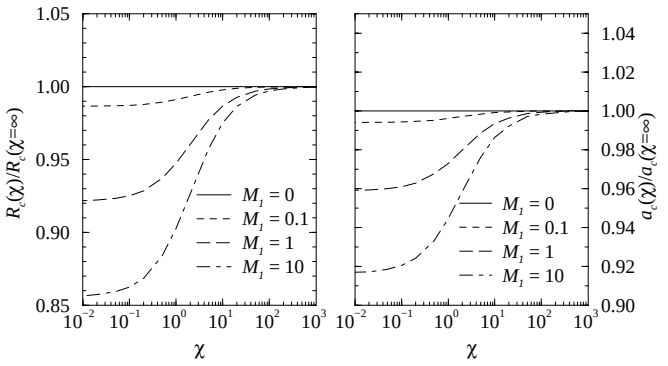

Fig. 5. At a constant ratio between the magnetic forces and buoyancy, the critical values (here for rigid boundaries) depend significantly on the susceptibility of the fluid.

This polynomial is bi-quintic, thus there are five independent contributions to the eigenfunctions of $\mathcal{L}$, *i.e.* $n = 5$. The constants w_j, t_j and f_j (as well as u_j and v_j, which are the equivalents for $U(z)$ and $V(z)$, respectively) are determined by $\mathcal{L}u = 0$:

$$f_j = 1 \tag{44}$$

$$t_j = -\frac{q_j^2 - a^2 M_3}{q_j} \coth\left(\frac{q_j}{2}\right) \tag{45}$$

$$w_j = (q_j^2 - a^2) t_j \tag{46}$$

$$u_j = \frac{\mathrm{i} q_j}{a} \tanh\left(\frac{q_j}{2}\right) w_j \tag{47}$$

$$v_j = -\mathrm{i}\frac{aR\left[(1+M_1)t_j \tanh\left(\frac{q_j}{2}\right) + M_1 q_j\right]}{\sqrt{T} q_j} - \mathrm{i}\frac{(q_j^2 - a^2)^3 t_j \tanh\left(\frac{q_j}{2}\right)}{\sqrt{T} q_j} \,. \tag{48}$$

Once again we omit all unnecessary functions in the following. Comparison of u_j and v_j shows again the effect of the Taylor-Proudman theorem. Inserting the characteristic polynomial in v_j reveals that v_j is proportional to $\sqrt{T}$ as for free boundaries. Inserting the solution of $\mathcal{L}u = 0$ into the boundary conditions leads to a system of six coupled linear equations for the coefficients B_j. The solvability condition for them gives the neutral curve and solving them explicitly one obtains the constants B_j and the solutions of $\mathcal{L}u = 0$ for rigid boundaries. Since we have to compute the roots of the characteristic polynomial numerically, there is no analytic expression for the neutral curve. Minimization of the neutral curve gives the critical values for rigid boundaries. An overview of the result can be found in Figure 4. If not mentioned explicitly, in all calculations for rigid boundaries we assume the susceptibility of the fluid to be $\chi = 2$. As in the free boundary case, the two regimes at low and high rotation rates appear.

Using the same procedure to solve the equations, we searched for an oscillatory instability for rigid boundaries. In all investigated cases we can exclude such an instability, given that the Prandtl number is larger than unity (for all magnetic fluids currently available).

3.2.3 Dependence of the critical values on the susceptibility

Independent of the magnetic parameters M_1 and M_3, the susceptibility χ enters the governing equations *via* the magnetic boundary conditions. Varying the susceptibility of the fluid (but keeping the other parameters constant) has a significant influence on the critical values. In Figure 5 we plot the Rayleigh number and the wave number as ratios between their critical values at a certain finite χ and $\chi \to \infty$, for the case of rigid boundary conditions.

Using the method of solution described for rigid boundaries we can drop the assumption $\chi \to \infty$ in the free boundary case. The variation of the critical values here is more important than for rigid boundaries (R_c is reduced by approximately 25%), but the overall form of the curves is the same as in Figure 5. This illustrates another limitation of the applicability of the analytic calculations for free boundaries (in Sect. 3.1 we already discussed the Rosensweig instability). The critical values for realistic susceptibilities differ significantly from those for $\chi \to \infty$.

3.3 Comparison of the above results to asymptotic solutions

3.3.1 Large rotation rates

Expanding the linear equations for free boundaries in the limiting case $T \to \infty$ leads to the following equation for the z-dependence of v_z:

$$\left[-a^6 + T\partial_{zz} + a^2 R(1+M_1)\right] W = 0. \tag{49}$$

In accordance with the boundary conditions this equation can be solved by a cos-ansatz, which leads to the following expression for the neutral curve:

$$R' := R(1+M_1) = a^4 + \pi^2 \frac{T}{a^2} \,. \tag{50}$$

Table 4. Comparison of the power laws for the critical values at large the Taylor numbers ($a_c = a_0\, T^\gamma$, $R_c = R_0\, T^\delta$) with a fit for $T > 10^7$ to the exact results.

boundaries		fit	power law
free	R_0	8.8	8.696
	δ	0.666	$\frac{2}{3}$
	a_0	1.305	1.3048
	γ	0.16667	$\frac{1}{6}$
rigid	R_0	5.82	8.696
	δ	0.677	$\frac{2}{3}$
	a_0	0.984	1.3048
	γ	0.175	$\frac{1}{6}$

Thus the critical values are given by

$$a_c = \left[\frac{1}{2}\pi^2 T\right]^{\frac{1}{6}} \approx 1.3\, T^{\frac{1}{6}} \tag{51}$$

and

$$R_c' = 3\left[\frac{1}{2}\pi^2 T\right]^{\frac{2}{3}} \approx 8.7\, T^{\frac{2}{3}}. \tag{52}$$

Figures 3 and 4 show that these power laws are in good agreement with the results presented above (for both rigid and free boundaries). To emphasize this point further we compare these asymptotic results to fits for large T ($T > 10^7$) to our earlier results in Table 4. For free boundaries the fitted values are almost indistinguishable from the asymptotic predictions. Rigid boundaries seem to be more constraining for the system and so there are still some small differences between the asymptotic exponents and the fitted values for all used values of the Taylor number. The differences in the prefactors reflect the influence of the boundary conditions on the critical values.

From equation (50) it follows also that the critical Rayleigh number, scaled by a factor $(1 + M_1)$, should be independent of M_1 at large T. In Table 5 we show, that the scaling factors needed to superpose the curves of $R_c(T)$ for different M_1 are indeed very close to $(1 + M_1)$.

3.3.2 Heating from above

As mentioned in Section 2 the Kelvin force also acts to destabilize the layer if it is heated from above (see also [19,23]). In our formulation, heating from above is expressed by a negative β and thus a negative R. This implies also M_1 to be negative, since all physical constants belonging to only one of the two parameters are strongly positive. For M_1 being the ratio between the Kelvin force and buoyancy, convection is only possible for $M_1 < -1$, *i.e.* the destabilizing force (Kelvin) must exceed the stabilizing force (buoyancy). In the limit $M_1 \to -1$ both the critical wave number and the critical Rayleigh number grow rapidly (see also [23]).

Table 5. Comparison of the shift factors to the critical Rayleigh numbers, which allow the curves of Figures 3 and 4 coincide in one curve for free and rigid boundaries.

boundaries	M_1	fit	$1 + M_1$
free	0.1	1.09986	1.1
	1	1.9987	2
	10	10.987	11
rigid	0.1	1.0987	1.1
	1	1.9964	2
	10	10.973	11

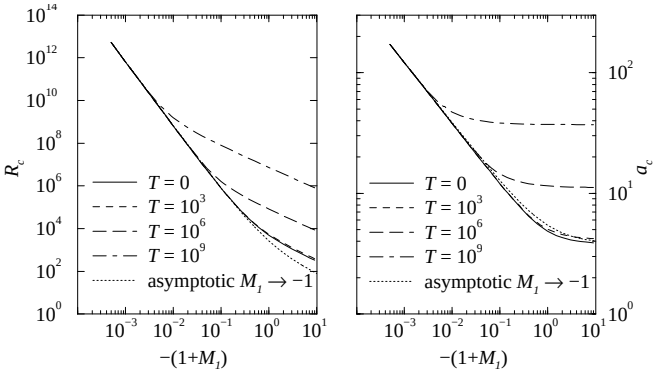

Fig. 6. The critical values in the regime $M_1 \to -1^-$ for rigid boundary conditions. See text for a detailed discussion.

Supposing free boundary conditions and power laws of the form

$$a_c = a_0(-1 - M_1)^\gamma \tag{53}$$

for the critical values in the region of $M_1 \approx -1$ we find the asymptotic differential equation

$$\left[a^8 M_3 - a^4 R(1 + M_1)M_3 + a^2 R M_1 \partial_{zz}\right] W(z) = 0 \tag{54}$$

for the vertical component of the velocity field. The usual cos-ansatz leads directly to the asymptotic expressions

$$a_c^2 = \frac{3}{2}\ \frac{M_1}{1 + M_1}\ \frac{\pi^2}{M_3} \tag{55}$$

$$R_c = \frac{27}{4}\pi^4 \left(\frac{M_1}{M_3}\right)^2 \frac{1}{(1 + M_1)^3} \tag{56}$$

determining the critical values. In Figure 6 we compare the asymptotic results to the results of the full equations as presented in Section 3.2.2. Note, that the asymptotic solution was determined for free boundary conditions, but is also a very good approximation for the rigid case. No adjustment of the prefactors (as for the large T limit) was necessary here.

4 Weakly nonlinear analysis

4.1 Mathematical formulation and method of solution

4.1.1 Expansion in a small parameter

To describe the system operating slightly above the critical Rayleigh number, we perform a weakly nonlinear analysis following the lines of Schlüter, Lortz and Busse [2]. A recent overview of weakly nonlinear analysis on rotating convection in simple fluids is given by Clune and Knobloch [7]. With the small parameter

$$\epsilon^2 = \frac{R - R_\mathrm{c}}{R} \tag{57}$$

we expand all functions in ϵ and assume that all variations of the linearized solutions can be incorporated into an amplitude function A.

$$u \to \epsilon A \left[u^{(0)} + \epsilon u^{(1)} + \epsilon^2 u^{(2)} + O(\epsilon^3) \right]. \tag{58}$$

Here $u^{(0)}$ is the linear solution determined in the previous section. Inserting (58) into the governing equations, we can expand these equations in orders of ϵ and obtain the hierarchy of equations

$$\epsilon^1 \colon \mathcal{L}^{(0)} u^{(0)} = 0 \tag{59}$$

$$\epsilon^2 \colon \mathcal{L}^{(0)} u^{(1)} = -\mathcal{N}(u^{(0)}|u^{(0)}) \tag{60}$$

$$\epsilon^3 \colon \mathcal{L}^{(0)} u^{(2)} = -\mathcal{L}^{(2)} u^{(0)} - \mathcal{N}(u^{(0)}|u^{(1)}) - \mathcal{N}(u^{(1)}|u^{(0)}). \tag{61}$$

These equations must be solved iteratively each time fulfilling the solvability condition

$$\langle u^+ | r.h.s. \rangle = 0, \tag{62}$$

where u^+ is the solution to the linear adjoint problem (see below), $r.h.s.$ is the corresponding right hand side of equations (59) through (61) and $\langle \cdot \rangle$ denotes the average over a suitable volume. This solvability condition is trivially satisfied in order ϵ. In order ϵ^2 a mere integration over the horizontal coordinates shows that (62) is fulfilled, since u^+ and $\mathcal{N}(u^{(0)}|u^{(0)})$ contain different exponential functions. But (62) leads to an equation for the amplitude A in ϵ^3 of the type [7,34,35]

$$\tau_0 \partial_t A = \left[\epsilon^2 + \xi_0^2 \partial_{xx} - g|A|^2 \right] A. \tag{63}$$

The coefficients of this equation are [7,35]:

$$\tau_0 = \left(R_\mathrm{c} \frac{\partial \lambda}{\partial R} \right)^{-1} \Bigg|_{R_\mathrm{c}} \tag{64}$$

$$\xi_0^2 = \frac{1}{2R_\mathrm{c}} \frac{\partial^2 R}{\partial a^2} \Bigg|_{R_\mathrm{c}} \tag{65}$$

$$g = \left[\left(R_\mathrm{c} \frac{\partial \lambda}{\partial R} \right)^{-1} \langle u^+ | \mathcal{N}(u^{(0)}|u^{(1)}) + \mathcal{N}(u^{(1)}|u^{(0)}) \rangle \right]_{R_\mathrm{c}}. \tag{66}$$

For plots of these coefficients see Section 4.2.

4.1.2 Adjoint system

To determine the adjoint system of equations we make use of the identity

$$\langle u^+ | \mathcal{L} u \rangle = \langle \mathcal{L}^+ u^+ | u \rangle. \tag{67}$$

Thus the adjoint system can be calculated *via* integration by parts of the governing equations. $\mathcal{L}^+$ is obtained by transposing $\mathcal{L}$ and replacing z by $-z$. Special attention has to be paid to the boundary conditions of the adjoint system. They have to be chosen such that all integration constants vanish. We find that the adjoint boundary conditions for the velocity and the temperature are identical to equations (25) through (27), but the boundary conditions for the magnetic potential have to be replaced by

$$\phi^+ \left(z = \pm \frac{1}{2} \right) = (1 + \chi) \phi_\mathrm{e}^+ \left(z = \pm \frac{1}{2} \right) \tag{68}$$

$$\partial_z \phi^+ \left(z = \pm \frac{1}{2} \right) = \partial_z \phi_\mathrm{e}^+ \left(z = \pm \frac{1}{2} \right). \tag{69}$$

Using these boundary conditions we obtain the adjoint solutions u^+ following the same procedure as for $u^{(0)}$.

4.1.3 Construction of the nonlinear solution

We solve equation (60) in two steps: First we determine a special solution of the inhomogeneous system ignoring the boundary conditions. Then we add a solution of the homogeneous problem (with the appropriate symmetry — the opposite of the linear solution) to satisfy the boundary conditions. The ansätze for $u^{(1)}$ are given by the structure of $\mathcal{N}(u|u)$. We use

$$\sum_{i,j=1}^{5} C_{ij} \frac{\sinh(q_i z)}{\sinh\left(\frac{q_i}{2}\right)} \frac{\cosh(q_j z)}{\cosh\left(\frac{q_j}{2}\right)} \tag{70}$$

for odd and

$$\sum_{i,j=1}^{5} \left[D_{ij} \frac{\sinh(q_i z)}{\sinh\left(\frac{q_i}{2}\right)} \frac{\sinh(q_j z)}{\sinh\left(\frac{q_j}{2}\right)} + E_{ij} \frac{\cosh(q_i z)}{\cosh\left(\frac{q_i}{2}\right)} \frac{\cosh(q_j z)}{\cosh\left(\frac{q_j}{2}\right)} \right] \tag{71}$$

for even functions. The constants C_{ij}, D_{ij} and E_{ij} are different for each function. Inserting these ansätze in equation (60) leads to a system of linear equations for all C_{ij}, D_{ij} and E_{ij} which we solve *via* singular value decomposition numerically. The so constructed special solution of equation (60) — the special solution of the inhomogeneous system plus the homogeneous solution necessary to satisfy the boundary condition — is the solution $u^{(1)}$ which enters equation (66).

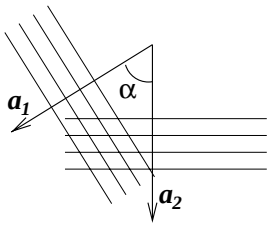

Fig. 7. When the KL instability sets in, the convection rolls with the wave vector $\mathbf{a}_1$ become unstable with respect to convection rolls rotated by an angle α.

4.1.4 Küppers-Lortz instability: two competing amplitudes

For simple fluids it is known [2,36,37] that straight rolls are stable just above the onset of convection if the rotation rate does not exceed the critical value for the onset of the KL instability. For the non-rotating case this has also been shown for magnetic fluids with free boundary conditions [26]. Following these results we consider the competition between two sets of convection rolls to investigate the Küppers-Lortz instability. Thus we will now investigate under which conditions a roll solution becomes unstable with respect to a rotated roll solution (both with the critical wave number) as schematically shown in Figure 7. To do this we extend the above described method of solution by ansätze of the type

$$u(x,y,z) = [A_1 u_1(z)\exp(\mathrm{i}\mathbf{a}_1\cdot\mathbf{r}) + A_2 u_2(z)\exp(\mathrm{i}\mathbf{a}_2\cdot\mathbf{r})] + \text{c.c.}, \quad (72)$$

with two independent amplitudes A_1 and A_2 corresponding to the roll solutions with the wave vectors $\mathbf{a}_1$ and $\mathbf{a}_2$ (with $|\mathbf{a}_1| = |\mathbf{a}_2| = a_\mathrm{c}$). Proceeding with these ansätze in the same way as above, *i.e.* expanding u_1 and u_2 in powers of ϵ and solving the resulting equations iteratively leads to two coupled amplitude equations.

$$\tau_0\partial_t A_1 = \left[\epsilon^2 + \xi_0^2\partial_{x_1x_1} - g|A_1|^2 - g_\alpha|A_2|^2\right] A_1 \quad (73)$$

$$\tau_0\partial_t A_2 = \left[\epsilon^2 + \xi_0^2\partial_{x_2x_2} - g|A_2|^2 - g_{\overline{\alpha}}|A_1|^2\right] A_2. \quad (74)$$

Here the coordinates x_1 and x_2 are along the direction of the wave vectors $\mathbf{a}_1$ and $\mathbf{a}_2$, respectively, $x_i = \mathbf{a}_i\cdot\mathbf{r}$. The coefficients τ_0, ξ_0 and g are identical to equations (64) through (66) if one just takes the terms into account which contain only one amplitude (either A_1 or A_2). The coupling constants g_α and $g_{\overline{\alpha}}$ are given by

$$g_\alpha = \left[\left(R_\mathrm{c}\frac{\partial\lambda}{\partial R}\right)^{-1}\langle u_1^+|\mathcal{N}(u^{(0)}|u^{(1)}) + \mathcal{N}(u^{(1)}|u^{(0)})\rangle\right]_{R_\mathrm{c}} \quad (75)$$

and

$$g_{\overline{\alpha}} = \left[\left(R_\mathrm{c}\frac{\partial\lambda}{\partial R}\right)^{-1}\langle u_2^+|\mathcal{N}(u^{(0)}|u^{(1)}) + \mathcal{N}(u^{(1)}|u^{(0)})\rangle\right]_{R_\mathrm{c}}, \quad (76)$$

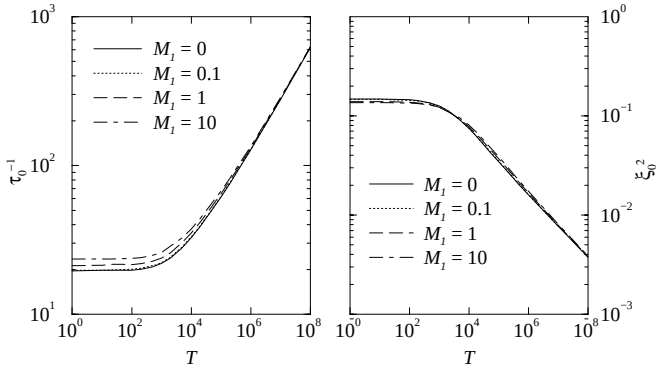

Fig. 8. The linear coefficients appearing in the amplitude equations (left τ_0^{-1} and right ξ_0^2) as discussed in the text.

where u_1^+ and u_2^+ are the solutions of the adjoint system with the wave vectors $\mathbf{a}_1$ and $\mathbf{a}_2$ respectively. In the expressions for g_α and $g_{\overline{\alpha}}$ only terms containing both amplitudes must be taken into account.

Bifurcation theory leads to some important results (see *e.g.* [7]): If $g > 0$ the bifurcation is forward. Equations (73, 74) allow one to determine the range in which single mode convection (*e.g.* $A_1 \neq 0$ and $A_2 = 0$) is stable against perturbations of the second mode (A_2). Suppose we have a situation where one amplitude is zero and the other is non zero. The mode with the vanishing amplitude can only grow if the coefficient of the cross coupling term (g_α or $g_{\overline{\alpha}}$) is smaller than the coefficient of the nonlinear damping term (g) — provided we take the sign convention used in equations (73, 74). Thus, A_1 is unstable to A_2 if $g > g_{\overline{\alpha}}$, and A_2 is unstable to A_1 if $g > g_\alpha$. In the first case the convection pattern seems to rotate in the direction of the applied rotation, in the second case the pattern seems to rotate against this direction.

4.2 Results and discussion

In Figure 8 the linear coefficients of the amplitude equations are given.

The curves for $M_1 = 0$ agree with the results for simple fluids [7] and increasing the contribution of the magnetic force (M_1) does not change the overall behavior. The other magnetic parameters were fixed at $M_3 = 1.1$ and $\chi = 2$. We do not present the nonlinear coefficients here, since they depend on the normalization of the amplitude functions. But nevertheless we want to point out that g is always positive, *i.e.* the bifurcation is forward as in the simple fluid case. In Figure 9 we show the difference $g_{\overline{\alpha}} - g$ for Taylor numbers below and above the critical value. g_α is always larger than g, thus the pattern rotates in the direction of the external rotation.

In Figure 10 we present the dependence of the KL angle on M_1. The KL angle predicted for convection including a magnetic force is always greater than for a simple fluid with the same Prandtl number (results for $M_1 = 0$). For large absolute values of M_1, the curves seem

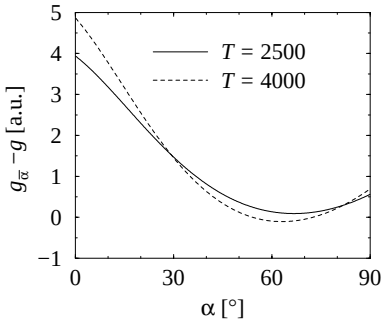

Fig. 9. The difference between the nonlinear terms in the amplitude equation for the magnetic parameters $M_1 = 2$ and $M_3 = 1$ and Taylor numbers near the critical value ($T_c = 3234.76$).

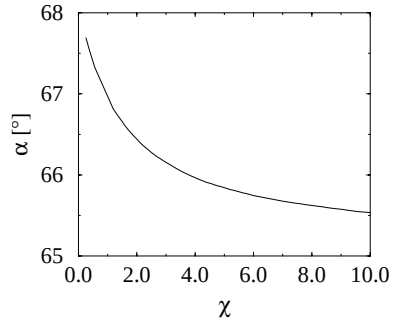

Fig. 11. The KL angle increases with decreasing susceptibility (holding the other magnetic parameters constant). For this plot we used $M_1 = 10$, $M_3 = 1$ and $P = 100$.

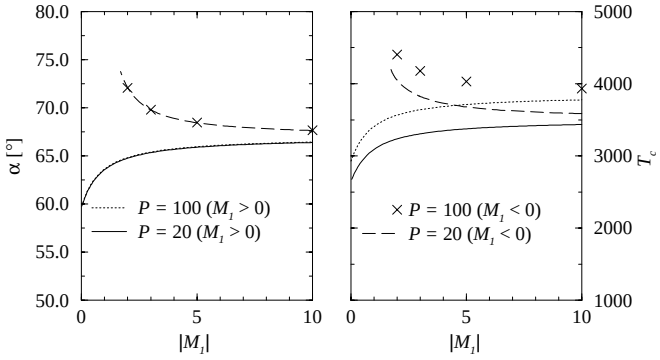

Fig. 10. The angle α between the initial and the final convection pattern in the KL instability (left) and the corresponding critical Taylor number, above which the KL instability sets in. The solid and dotted curves correspond to the cell heated from below ($M_1 > 0$), the dashed curves to heating from above ($M_1 < 0$).

to approach a common value which does not depend on the sign of M_1 but only on the Prandtl number. This behavior can be easily understood since the magnetic parts of the governing equation do not depend on the sign of M_1 (if M_1 is negative also R is negative). This implies that magnetically dominated convection does not distinguish between a system heated from above or below. Thus we expect the KL angle to be independent of the sign of M_1 for large absolute values of M_1. The variation of the KL angle at the largest values of M_1 used shows that buoyancy is not yet negligible. As in the simple fluid case, the KL angle does not vary significantly for Prandtl numbers between 20 and 100. As shown in Figure 11 the KL angle increases even further if the susceptibility of the fluid decreases.

In summary, we have reported a well controlled way of changing the KL angle continuously in thermal convection in a magnetic fluid between the value corresponding to a simple fluid (approximately 60° for Prandtl numbers typical for magnetic fluids), to almost 75° by increasing the contribution of the magnetic forces. This makes a range of KL angles accessible just by tuning a continuously variable parameter, the magnetic field. This would not be accessible using simple fluids.

GKA thanks W. Pesch and J. Weilepp for interesting and stimulating discussions. We thank the Deutsche Forschungsgemeinschaft for partial support of this work through the Graduiertenkolleg “Nichtlineare Spektroskopie und Dynamik”.

References

1. S. Chandrasekhar, *Hydrodynamic and Hydromagnetic Stability* (Oxford University Press, New York, 1961).
2. A. Schlüter, D. Lortz, F. Busse, J. Fluid Mech. **23**, 129 (1965).
3. G. Küppers, D. Lortz, J. Fluid Mech. **35**, 609 (1969).
4. F.H. Busse, K.E. Heikes, Science **208**, 173 (1980).
5. F. Zhong, R. Ecke, V. Steinberg, Physica D **51**, 596 (1991).
6. E. Bodenschatz, D.S. Cannell, J.R. de Bruyn, R. Ecke, Y.-C. Hu, K. Lerman, G. Ahlers, Physica D **61**, 77 (1992).
7. T. Clune, E. Knobloch, Phys. Rev. E **47**, 2536 (1993).
8. L. Ning, R.E. Ecke, Phys. Rev. E **47**, 2991 (1993).
9. Y. Hu, R.E. Ecke, G. Ahlers, Phys. Rev. E **55**, 6928 (1997).
10. Y. Hu, W. Pesch, G. Ahlers, R.E. Ecke, Phys. Rev. E **58**, 5821 (1998).
11. K.M.S. Bajaj, J. Liu, B. Naberhuis, G. Ahlers, Phys. Rev. Lett. **81**, 806 (1998).
12. J.L. Neuringer, R.E. Rosensweig, Phys. Fluids **7**, 1927 (1964).
13. M.I. Shliomis, Sov. Phys.-Usp. **17**, 153 (1974).
14. R.E. Rosensweig, *Ferrohydrodynamics* (Cambridge University Press, London, 1985).
15. V.G. Bastovoy, B.M. Berkovsky, A.N. Vislovich, *Introduction to Thermomechanics of Magnetic Fluids* (Hemisphere Publishing Cooperation, Washington, 1987).
16. K. Henjes, M. Liu, Ann. Physics (N.Y.) **223**, 243 (1993).
17. B.A. Finlayson, J. Fluid Mech. **40**, 753 (1970).
18. K. Gotoh, M. Yamada, J. Phys. Soc. Jpn **51**, 3042 (1982).
19. L. Schwab, U. Hildebrandt, K. Stierstadt, J. Magn. Magn. Mat. **39**, 113 (1983).
20. L. Schwab, K. Stierstadt, J. Magn. Magn. Mat. **65**, 315 (1987).
21. L. Schwab, J. Magn. Magn. Mat. **85**, 199 (1990).
22. P.J. Stiles, M. Kagan, J. Colloid Interface Sci. **134**, 435 (1990).

23. P.J. Blennerhassett, F. Lin, P.J. Stiles, Proc. R. Soc. Lond. A **433**, 165 (1991).
24. P.J. Stiles, F. Lin, P.J. Blennerhassett, J. Colloid Interface Sci. **151**, 95 (1992).
25. C.L. Russel, P.J. Blennerhassett, P.J. Stiles, J. Magn. Magn. Mat. **149**, 119 (1995).
26. R. Bajaj, S.K. Malik, J. Math. Anal. Appl. **207**, 172 (1997).
27. J. Weilepp, H.R. Brand, J. Phys. II France **6**, 419 (1996).
28. M.D. Cowley, R.E. Rosensweig, J. Fluid Mech. **30**, 671 (1967).
29. D. Braithwaite, E. Beaugnon, R. Tournier, Nature **354**, 134 (1991).
30. J. Huang, B.F. Edwards, D.D. Gray, Phys. Rev. E **57**, R29 (1998).
31. P.J. Stiles, F. Lin, P.J. Blennerhassett, Phys. Fluids A **5**, 3273 (1993).
32. S. Odenbach, private communication, see also `http://www.tu-dresden.de/mw/ilr/hydromag/ferro/start.html` or `http://www.ferrofluidics.de/fluide/ferrofluid.html`
33. J. Huang, B.F. Edwards, Phys. Fluids **9**, 1819 (1997).
34. M.C. Cross, Phys. Fluids **23**, 1727 (1980).
35. Q. Feng, W. Pesch, L. Kramer, Phys. Rev. A **45**, 7242 (1992).
36. R.M. Clever, F.H. Busse, J. Fluid Mech. **94**, 609 (1979).
37. A.C. Newell, J.A. Whitehead, J. Fluid Mech. **38**, 279 (1969).